The Ventilated Thermocline[1]

J. R. LUYTEN, J. PEDLOSKY AND H. STOMMEL
Woods Hole Oceanographic Institution, Woods Hole, MA 02543

(Manuscript received 3 May 1982, in final form 24 August 1982)

ABSTRACT

A simple theoretical model for the oceanic thermocline and the associated field of currents is presented. The model consists of a finite but arbitrarily large number of inviscid, homogeneous fluid layers each with a different density. The dynamical balances everywhere are Sverdrupian. In regions where the Ekman pumping is negative (downward) the surface density is specified, i.e., the position of the outcrop of density interfaces is specified. This outcropping of density layers allows deep motion to be excited by the ventilation provided by Ekman pumping even in latitudes far south of the outcrop where the layer is shielded from direct influence of the wind. Analytical solutions are presented in the case where the density-outcrop lines are coincident with latitude circles. The solutions are not self-similar and important sub-domains of the solution are defined by critical potential vorticity trajectories which separate the ventilated from the unventilated regions in the lower thermocline. These critical trajectories also separate regions of strong variations in potential vorticity from regions of fairly weak variation in potential vorticity although the small variations in potential vorticity in the latter are crucial to the dynamics.

Comparison is made between the predictions of the model and data from the Atlantic with encouraging results.

1. Introduction

During the past 20 years considerable theoretical effort has been given to the problem of determining the vertical structure of the oceanic circulation. This is the problem of the thermocline and its considerable technical difficulty is already apparent in the earliest modern papers on the subject (e.g., Robinson and Stommel, 1959; Welander, 1959). The heart of the problem and its accompanying difficulty is the tendency of a weakly dissipative fluid to preserve both its density ρ and potential vorticity q over great distances from source areas of both fields. Since the vertical distributions of velocity and density in the ocean are controlled by these fields, and since ρ and q are carried great lateral distances by the fluid, the problem of the vertical structure of the thermocline is inescapably coupled to the horizontal structure of the oceanic circulation. The pathway along which fluid moves in a steady non-dissipative regime of flow is simply the trajectory of constant q on surfaces of constant ρ. In the interesting limit of an ideal fluid the problem then "reduces" to determining the three-dimensional potential vorticity trajectories on surfaces of constant density whose configurations are themselves determined by the flow.

It is therefore not to be wondered at that progress on this problem has been difficult and slow. To avoid the demanding difficulties associated with the three-dimensional nature of the basic physics, attempts were initially made to derive similarity solutions of the nonlinear partial differential equations that naturally arise in continuous models of the thermocline [see Veronis (1969) for a review of these attempts]. As Welander (1971) pointed out, relatively little physical insight has been gained from the similarity solutions. Not only are they deficient in terms of the boundary conditions they can satisfy but more fundamentally they depend on special balances of terms within the equations which collapse the physics and lead to highly constrained distributions of q (e.g., a constant on density surfaces). It seems likely that real physical insight will only occur in models that abandon the similarity hypothesis (which is unlikely to hold over the whole oceanic gyre in any case).

A companion conceptual difficulty associated with the largely technical difficulty described above also haunts the history of the thermocline problem. This is the dual question of determining how a fluid below the surface layer, directly driven by the wind, is set into motion, and what determines the depth to which that motion penetrates. In the absence of significant frictional stresses between fluid layers of a stratified fluid only the fluid immediately acted upon by the wind stress can be brought into motion. The existence of subsurface motion therefore requires either fluid trajectories that thread back to intersect near-surface regions directly affected by Ekman pumping or the

[1] W.H.O.I. Contribution No. 5146.

motions require momentum transfer by sub-gyre-scale mixing processes.

Consider, first, the second alternative. Imagine a layered model of the ocean in which the interfaces between the layers, though not level, *never* slope strongly enough to break through to the surface. We would term this an "unventilated ocean". If mixing is very weak, the potential vorticity will be conserved in each layer not immediately adjacent to the upper or lower horizontal surface. If the potential vorticity isopleths in each layer intersect an eastern oceanic boundary (which is envisioned as being incapable of supporting a flux into or out of a boundary layer), then the fluid will be motionless along the entire length of that potential vorticity contour. On the other hand, if these contours should close on themselves no such inhibition to motion around those contours occurs. Rhines and Young (1981) have explored this possibility in considerable detail and have shown how the effect of weak dissipation may lead to submerged, closed pools of constant potential vorticity bounded by these closed contours and containing motions considerably more vigorous than those which can occur on the "open" potential vorticity contours striking the eastern boundary. In this scheme deep motion of an unventilated ocean can occur only in domains bounded by closed potential vorticity contours and the motion within those contours is imagined to be driven by the small but relentless frictional coupling to upper layers. The frictional coupling, perhaps by eddies, then gives rise to potential vorticity fluxes which homogenize the potential vorticity within the bounding contour and provide the propulsive flow mechanism. Everywhere else, the unventilated fluid below the very uppermost layer is completely stagnant. It seems to us that the above picture depends in a most unrealistic way on the complete shielding of the lower layers from the surface region. The purpose of the present study, therefore, is to examine an alternative hypothesis. Namely, we imagine a layered system in which several layers intersect the upper surface where the fluid in the layers can be ventilated by water pumped down from the upper Ekman layer. We then trace the subsequent motion of these layers well into regions where they are shielded from direct wind forcing and in which their potential vorticity is conserved.

One major result of the study presented here is its demonstration of significant motion at depth on *open* potential vorticity contours that thread back to meet the ocean surface rather than the eastern boundary. [This allows us to avoid the catastrophic limitation of motion to unrealistically shallow regions which Rhines and Young (1981) demonstrate is a feature of an unventilated, potential vorticity conserving ocean.] The layered model is also simple enough to succumb to straightforward analytical methods so that thermocline solutions are easily found. Indeed the second major result of our analysis is the inevitability of distinct regions of flow not describable within a single similarity solution. In fact, we present solutions with four separate flow domains. In regions of Ekman downwelling the surface density distribution is prescribed. This region will be shown to break further into a three-fold subdivision. First, there exists a constantly refreshed, ventilated region in which all fluid layers are in motion. On the periphery of this ventilated region, shadow zones emerge traced by potential vorticity contours emerging from meridional boundaries. These shadow zones may bound regions of uniform potential vorticity or regions which are stagnant. The fourth zone occurs in regions of Ekman upwelling. The surface density field there is no longer arbitrarily prescribed. Instead density surfaces are pulled, one after another, to the surface in response to Ekman suction. More detailed discussion of our results and comparison with observation is best delayed until a presentation of our model and its analysis.

It is fair to point out that physically our model in many ways resembles the early ideal fluid model of Welander (1959), especially in its relationship between the existence of deep motion and ventilation. The major simplifications resulting from the layer formulation allow us to break free of constraints imposed by the demand for similarity solutions in the earlier theoretical studies and to examine solutions which are only partially ventilated.

2. The model

The physical model is shown in Fig. 1. Our model ocean consists of N layers with thickness h_1, h_2, $\ldots$, h_N which intersect the sea surface at latitudes y_j. The y_j are in general functions of longitude, i.e., $y_j = y_j(x)$. The density of each layer is a constant, ρ_j, $j = 1, \cdots N$. The layers are immiscible and all frictional coupling between the layers is ignored. The model is imagined to apply to the region below the surface mixed layer so that on the upper surface of the fluid shown in Fig. 1 the vertical velocity is prescribed, i.e.,

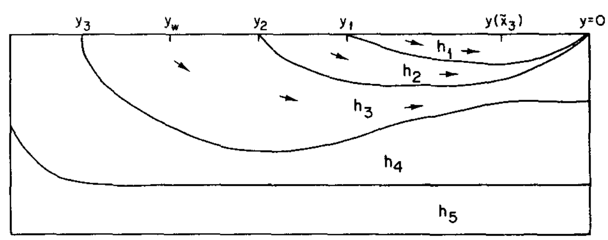

FIG. 1. A schematic meridional cross section of the model. The latitudes of the density outcrops are y_1, y_2 and y_3 as described in the text. The Ekman pumping changes sign at $y_w(x)$. South of $y(x_3)$ layer 3 is motionless.

$$w = w_e(x, y) \quad \text{on} \quad z = \eta(x, y), \tag{2.1}$$

where η is the elevation of the air-sea interface and w_e the Ekman pumping velocity. For simplicity and concreteness we limit our attention to the case where w_e is positive north of the line $y = y_w(x)$ and is negative between y_w and the equator (at $y = 0$).

Although the analysis given below can be done for an arbitrary number of layers we will henceforth only consider the case where at most three layers are exposed to the surface within $0 \leq y \leq y_w(x)$. Unless there are deep sources of inflow into layer 4 it is not difficult then to show that layer 4 and all deeper layers will be motionless for $y < y_w(x)$. Therefore in this southern region, which we think of as the classic anticyclonic, subtropical gyre, only three layers are in motion, with thicknesses h_1, h_2 and h_3.

We will insist that on the oceanic eastern boundary, which we take to be $x = x_E$, the geostrophic zonal flow must vanish. We momentarily defer a discussion of the layer configuration north of $y = y_w(x)$.

Our dynamical model is Sverdrupian. That is, within each layer the motion is geostrophic and hydrostatic, i.e., with standard notation

$$\left.\begin{aligned} \rho_n f u_n &= -\frac{\partial p_n}{\partial y} \\ \rho_n f v_n &= \frac{\partial p_n}{\partial x} \\ \rho_n g &= -\frac{\partial p_n}{\partial z} \end{aligned}\right\}, \tag{2.2a, b, c}$$

and incompressible

$$\frac{\partial u_n}{\partial x} + \frac{\partial v_n}{\partial y} + \frac{\partial w_n}{\partial z} = 0, \tag{2.3}$$

where $n = 1, 2, 3$, etc., labels the fields in layer n.

The Sverdrup vorticity equation obtained from (2.2a,b) and (2.3) is

$$\beta v_n = f \frac{\partial w_n}{\partial z}. \tag{2.4}$$

It is helpful to consider the following integrals of (2.4). When (2.4) is integrated over each layer and the resulting integrals are summed over all moving layers we obtain the Sverdrup relation

$$\beta \sum_n h_n v_n = f w_e(x, y). \tag{2.5}$$

At the same time if (2.4) is integrated over the depth of each layer, then in those regions where the layer is not directly exposed to the pumping from the Ekman layer, it follows that

$$u_n \frac{\partial}{\partial x} \frac{f}{h_n} + v_n \frac{\partial}{\partial y} \frac{f}{h_n} = 0. \tag{2.6}$$

That is, once a layer is shielded above from the direct action of the wind by an intervening layer, the shielded layer conserves its potential vorticity f/h_n. Again, note that the dynamics is Sverdrupian so that the relative vorticity is ignored with respect to f in (2.6).

We now consider the region $y_2 \leq y \leq y_w$. Integration of the hydrostatic equation (2.2c) coupled with the requirement that layer 4 remain at rest yields

$$\left.\begin{aligned} v_3 &= \frac{\gamma_3}{f} \frac{\partial}{\partial x} h_3 \\ u_3 &= -\frac{\gamma_3}{f} \frac{\partial}{\partial y} h_3 \end{aligned}\right\}, \tag{2.7a, b}$$

where $\gamma_3 = g(\rho_4 - \rho_3)/\rho_0$. We have also assumed that all density differences are slight compared to the average density ρ_0.

In $y_2 \leq y \leq y_w$ only one layer is in motion so that the Sverdrup relation (2.5) becomes (using 2.7a)

$$\frac{\partial}{\partial x} h_3^2 = \frac{2f^2}{\beta \gamma_3} w_e(x, y). \tag{2.8}$$

whose integral yields

$$h_3 = [D_0^2(x, y) + H_0^2]^{1/2}. \tag{2.9}$$

We have defined the function

$$D_0^2(x, y) = -\frac{2f^2}{\beta \gamma_3} \int_x^{x_E} w_e(x', y) dx', \tag{2.10}$$

which is positive for $y < y_w$. H_0 is a constant and it follows from (2.7b), (2.9) and (2.10) that $h_3 = H_0$ on $x = x_E$ so that the zonal flow will vanish there.

In this region $(y_2 < y < y_w)$

$$h_3 v_3 = \frac{f}{\beta} w_e < 0, \tag{2.11}$$

so that fluid columns are directly driven downward and southward. As they cross the line $y = y_2$ they are subducted and immediately become insulated from the Ekman pumping and thereafter preserve their potential vorticity.

In the region south of y_2 (but north of y_1) two layers are in motion; these are layers 2 and 3. Within layer 3 Eq. (2.6) applies. The hydrostatic relation in layer 3 now implies that

$$\left.\begin{aligned} v_3 &= \frac{\gamma_3}{f} \frac{\partial}{\partial x} H \\ u_3 &= -\frac{\gamma_3}{f} \frac{\partial H}{\partial y} \end{aligned}\right\}, \tag{2.12a, b}$$

where $H = h_2 + h_3$ is the *total* thickness of the fluid in motion. If (2.12a,b) is used in (2.6) it immediately follows that a first integral of (2.6) can be obtained as

$$\frac{f}{h_3} = G_3(H), \tag{2.13}$$

which restates the fact that the potential vorticity trajectories coincide with the isobars in layer 3. The function $G_3(H)$ is arbitrary. It can be determined, however, by noting that on $y = y_2$, where h_2 vanishes, $h_3 = H$. Thus noting that $f = f(y)$.

$$\frac{f(y_2)}{H} = G_3(H), \quad y = y_2(x). \tag{2.14}$$

In the general case where y_2 is a function of x we must first invert $y = y_2(x)$ to find x as a function of y at the position where h_2 vanishes. Then along that contour (2.9) can be used to find a one-to-one relation between $h_3 = H$ and y on $y_2(x)$. This allows $f(y_2)$ to be written as a function of H on $y = y_2(x)$, which determines the function $G_3(H)$. We outline this general inversion process mainly to argue that the analysis can proceed in principle regardless of the geometry of $y_2(x)$.

Note, however, that the characteristics of the partial differential equation (2.6) are the fluid trajectories in the horizontal plane. Thus care must be taken to eliminate the pathological case where $y_2(x)$ folds back to intersect a trajectory more than once. The problem once such complexities arise remains somewhat obscure.

For simplicity and the desirability of achieving simple concrete representations for the fields of motion, we present explicit solutions only for the case where y_1 and y_2 are lines of constant latitude. In that case (2.14) is simply

$$G_3(H) = \frac{f_2}{H},$$

where $f_2 \equiv f(y_2)$. Thus (2.13) yields the simple relation

$$\frac{f}{h_3} = \frac{f_2}{H}, \tag{2.15}$$

so that in $y_1 \leq y \leq y_2$,

and, therefore,
$$\left.\begin{aligned} h_3 &= \frac{f}{f_2} H \\ h_2 &= (1 - f/f_2)H \end{aligned}\right\}. \tag{2.16a, b}$$

It is very important to remember that (2.16a,b) holds only for those (x, y) points which can be traced back to y_2 along a potential-vorticity trajectory in layer 3. All columns initially at $y = y_2$ will move southward but not all points south of y_2 in layer 3 will necessarily be hit by a potential vorticity trajectory. We return to this important point below.

Within layer 2 the hydrostatic equation implies that

$$\left.\begin{aligned} v_2 &= \frac{1}{f}\frac{\partial}{\partial x}(\gamma_3 H + \gamma_2 h_2) \\ u_2 &= -\frac{1}{f}\frac{\partial}{\partial y}(\gamma_3 H + \gamma_2 h_2) \end{aligned}\right\}, \tag{2.17}$$

where $\gamma_2 = g(\rho_3 - \rho_2)/\rho_0$, so that the Sverdrup relation (2.5) in $y_1 \leq y \leq y_2$ becomes

$$\frac{\partial}{\partial x}\left(H^2 + \frac{\gamma_2}{\gamma_3} h_2{}^2\right) = \frac{2f^2}{\beta\gamma_3} w_e(x, y), \tag{2.18}$$

whose integral is

$$H^2 + \frac{\gamma_2}{\gamma_3} h_2{}^2 = D_0{}^2(x, y) + H_0{}^2. \tag{2.19}$$

In (2.19) we have anticipated the result that the constant of integration must, by continuity of h_2, match the constant in (2.9) so that on $x = x_E$ at $y = y_2$,

$$H = h_3 = H_0$$

as y_2 is approached from the north or south. It then follows from (2.16b) that

$$H = \frac{(D_0{}^2 + H_0{}^2)^{1/2}}{\left[1 + \frac{\gamma_2}{\gamma_3}(1 - f/f_2)^2\right]^{1/2}}, \tag{2.20}$$

from which h_2, h_3, and the corresponding geostrophic velocities are immediately determined. Note, however, that the layer-thickness ratio $h_2/h_3 = [(f_2/f) - 1]$ is independent of both the forcing w_e and the density difference between the layers, and depends only on distance from the outcrop latitude.

Now, we first suppose that (2.20) holds directly up to the ocean's eastern boundary (where D_0 vanishes). In order for u_3 and u_2 to vanish on x_E it follows that both H and h_2 must be constant along $x = x_E$. Noting (2.16b), this requires both

$$\left.\begin{aligned} &\frac{\partial H}{\partial y} = 0 \\ &\frac{\partial}{\partial y}(1 - f/f_2)H = 0 \end{aligned}\right\}$$

on $x = x_E$, which in turn demands that H vanish on $x = x_E$ or equivalently that $H_0 = 0$. If H_0 is zero the total depth of the moving region goes to zero at the eastern wall. In only that case will (2.20) be valid right up to $x = x_E$.

From a strictly theoretical viewpoint such a solution seems much too special for, in principle at least, some condition on the *overall* depth of the warm water region at $x = x_E$ should be free rather than determined by kinematic boundary conditions. Furthermore, the observational evidence described in Section 3 supports the notion that H_0 really ought not to be zero, i.e., that the eastern boundary is in contact with warmer thermocline water. How then is the conundrum posed by the eastern boundary condition to be met?

We now consider the trajectory of a fluid column in layer 3 that is subducted at the point (ξ, y_2). It traverses a path of constant f/h_3 which is also a path of constant H[(2.15)]. The resulting path is then given implicitly by the relation $H(x, y) = H(\xi, y_2)$, or

$$D_0^2(x, y) = D_0^2(\xi, y_2)\left[1 + \frac{\gamma_2}{\gamma_3}(1 - f/f_2)^2\right] + \frac{\gamma_2}{\gamma_3} H_0^2(1 - f/f_2)^2. \quad (2.21a)$$

We let ξ approach the eastern boundary where D_0^2 vanishes for all y. The trajectory $\tilde{x}_3(y)$ (see Fig. 2) emanating from this point is given by $H(\tilde{x}_3, y) = H(x_E, y_2) = H_0$ or,

$$D_0^2(\tilde{x}_3, y) = \frac{\gamma_2}{\gamma_3} H_0^2(1 - f/f_2)^2. \quad (2.21b)$$

If H_0 is chosen to be zero, $\tilde{x}_3(y)$ will equal x_E for all $y < y_2$ and the trajectory will hug the eastern boundary. Otherwise, for all $H_0 \neq 0$ the trajectory emanating from (x_E, y_2) must swerve westward [since D_0^2 is an increasing function of $(x_E - x)$ for all $y < y_2$]. The physical reason for this separation is quite simple. Along the eastern boundary all layer thicknesses must be constant to avoid a zonal thermal wind current at $x = x_E$. But if the layer thickness is constant on the eastern boundary a column of fluid flowing southward along the boundary would be continuously reducing its potential vorticity whereas in fact its potential vorticity must be conserved. The resulting trajectory then enters the fluid interior searching out a potential vorticity isopleth. If H_0 is zero, h_3 vanishes on x_E, and columns on the eastern boundary possess an infinite store of potential vorticity, in that case alone can they flow parallel to the eastern boundary at $x = x_E$ and conserve potential vorticity.

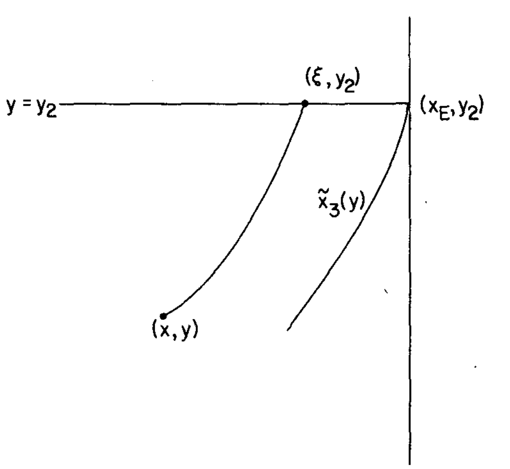

FIG. 2. In layer 3 the point (x, y) on a geostrophic trajectory is connected by the indicated contour to its origin at the point of subduction (ξ, y_2) is also shown.

Thus for $H_0 \neq 0$, $x_E - \tilde{x}_3(y) > 0$ for all $y < y_2$. The trajectory emanating from (x_E, y_2) separates the gyre into (at least) two regions. To the west of $\tilde{x}_3(y)$ both layers are in motion and that motion is determined by the memory of the potential vorticity each column of layer 3 has as it slips under the blanket of layer 2 at $y = y_2$. East of $\tilde{x}_3(y)$ no potential vorticity trajectory from $y = y_2$ can ventilate layer 3, and, in particular, Eq. (2.15) is no longer apt for $x > \tilde{x}_3(y)$. The shadow region carved out by $\tilde{x}_3(y)$ in layer 3 is bounded on the east by the eastern wall through which no fluid penetrates and on the west by the streamline $\tilde{x}_3(y)$. The depth of layer 3 is H_0 on both these boundary curves. Since this shadow region within layer 3 is not driven by either surface Ekman pumping or inflow across $\tilde{x}_3(y)$ or x_E, it seems natural to propose that this region is stagnant, i.e., $u_3 = v_3 = 0$. It is important to emphasize that in principle this is an arbitrary decision of ours, partly guided by observational evidence to be presented in Section 4.

Now along $\tilde{x}_3(y)$ H equals H_0. If this region of layer 3 is stagnant then H must equal H_0 for all x and y within the shadow region defined by $\tilde{x}_3(y)$. To complete the solution the Sverdrup relation (2.5) must be applied to the only moving layer, layer 2, i.e.,

$$\gamma_2 \frac{\partial h_2^2}{\partial x} = \gamma_3 \frac{\partial D_0^2}{\partial x},$$

or

$$h_2^2 = \frac{\gamma_3}{\gamma_2}(D_0^2 + \bar{h}^2), \quad (2.22)$$

where $\bar{h}$ is a constant. Now on $x = \tilde{x}_3(y)$ we insist on continuity of H and h_2 (and therefore h_3). H is trivially already continuous. Continuity of h_2 on $\tilde{x}_3(y)$ requires that

$$h_2(\tilde{x}_{3-}, y) = \left(1 - \frac{f}{f_2}\right)H_0 = h_2(\tilde{x}_{3+}, y) = \left[\frac{\gamma_3}{\gamma_2}(D_0^2(\tilde{x}_{3-}, y) + \bar{h}^2)\right]^{1/2}, \quad (2.23)$$

where $\tilde{x}_{3+}$ and $\tilde{x}_{3-}$ refer to points immediately to the east and west of $\tilde{x}_3(y)$, respectively. Examination of (2.21) shows that (2.23) requires that $h = 0$. That is, complete continuity across $\tilde{x}_3(y)$ is assured, but the upper layer must surface at the eastern boundary.[2] This must clearly occur since h_2 must be constant along x_E and it vanishes at $y = y_2$.

[2] Of course upwelling or downwelling on the eastern boundary will force a non-zero zonal geostrophic velocity in the upper layer and in such cases $h_2(x_E, y)$ need not vanish. We do not consider that elaboration of the theory here.

Thus for $x \leqslant \tilde{x}_3(y)$, Eqs. (2.16) and (2.20) describe the solution. In the unventilated, stagnant shadow region east of $\tilde{x}_3(y)$ the solution is described by

$$\left.\begin{aligned} h_2 &= \left(\frac{\gamma_3}{\gamma_2}\right)^{1/2} D_0(x, y) \\ h_3 &= H_0 - \left(\frac{\gamma_3}{\gamma_2}\right)^{1/2} D_0(x, y) \end{aligned}\right\} . \qquad (2.24\text{a,b})$$

It is important to note that the boundary between the region of validity of the solution given by (2.16) and (2.20) and the solution given by (2.24) is $\tilde{x}_3(y)$ in each layer, although only in the lower layer will $\tilde{x}_3(y)$ separate moving from stagnant fluid. The question is whether $\tilde{x}_3(y)$ is limited to some narrow zone in latitude near $y = y_2$ or whether it significantly penetrates southward. That is, how much of the lower layer really is ventilated? We will examine a specific example below (see Fig. 6). However some general remarks can be made here. If $\tilde{x}_3(y)$ is to penetrate southward the isopleths of potential vorticity in the ventilated zone must depart significantly from lines of constant latitude. Equivalently $\partial(f/h_3)/\partial x$ must be $O(\beta/h_3)$. From (2.20) and (2.10),

$$\frac{\partial}{\partial x} f/h_3 \approx \frac{f^3}{\beta\gamma_3} \frac{w_e}{H^3} .$$

To be as large as $O(\beta/h_3)$ this requires

$$H = O\left(\frac{f^3}{\gamma_3\beta^2} w_e\right)^{1/2}, \qquad (2.25)$$

which, with a slight change of notation is precisely the "advective scale" introduced by Welander (1971). Or, equivalently, it requires that w_e must exceed a value given by

$$w_e = \frac{\gamma_3\beta^2}{f^3} H^2.$$

With $f = 10^{-4}\ \mathrm{s}^{-1}$, $\beta = 10^{-13}\ \mathrm{cm}^{-1}\ \mathrm{s}^{-1}$, $\gamma_3 = 1$ and $H = 800$ m, a value of w_e of $6.4 \times 10^{-5}\ \mathrm{cm\ s}^{-1}$ is required which is of the order of commonly quoted values for subtropical Ekman pumping rates. It seems sensible then to conclude *a priori* that a significant region of the subtropical gyre can be ventilated from the outcropped isopycnal region.

The solution described above is valid in $y_1 \leqslant y \leqslant y_2$. South of y_1 the model contains three layers that may be in motion. The solution south of y_1 splits into three separate pieces. Reference to Fig. 3 shows that the separation trajectory $\tilde{x}_3(y)$ hits y_1 at the point x_* which by (2.20) is given by

$$D_0^2(x_*, y) = H_0^2 \frac{\gamma_2}{\gamma_3} (1 - f_1/f_2)^2. \qquad (2.26)$$

The three separate regions shown in Fig. 3 correspond to the following. Region L corresponds to a ventilated

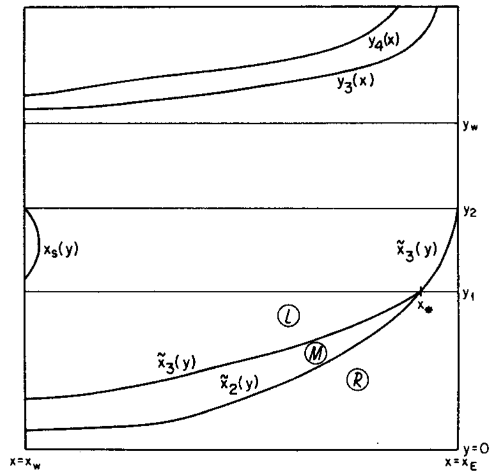

FIG. 3. A schematic showing the various domains of the solution in plan view.

region wherein all layers are in motion and all potential vorticity trajectories in layers 2 and 3 sweep in from $x < x_*$ on $y = y_1$. Region R has layer 3 motionless while the potential vorticity in layer 2 is swept in from the region $x > x_*$. The middle region M also has a stagnant layer 3 but in M information for layer 2 assigned at the point of subduction of layer 2 on $y = y_2$ comes from the solution region to the *left* of x_*.

South of $y = y_1$ the hydrostatic equation allows the horizontal velocities in the three layers to be written

$$\left.\begin{aligned} f\begin{pmatrix} u_1 \\ v_1 \end{pmatrix} &= \begin{pmatrix} -\dfrac{\partial}{\partial y} \\ \dfrac{\partial}{\partial x} \end{pmatrix} [\gamma_3 H + \gamma_2(h_1 + h_2) + \gamma_1 h_1] \\ f\begin{pmatrix} u_2 \\ v_2 \end{pmatrix} &= \begin{pmatrix} -\dfrac{\partial}{\partial y} \\ \dfrac{\partial}{\partial x} \end{pmatrix} [\gamma_3 H + \gamma_2(h_1 + h_2)] \\ f\begin{pmatrix} u_3 \\ v_3 \end{pmatrix} &= \begin{pmatrix} -\dfrac{\partial}{\partial y} \\ \dfrac{\partial}{\partial x} \end{pmatrix} \gamma_3 H \end{aligned}\right\} \qquad (2.27\text{a, b, c})$$

where $\gamma_1 = g(\rho_2 - \rho_1)/\rho_0$.

In region L the potential vorticity conservation statements for layers 2 and 3 are, respectively,

$$\left.\begin{aligned} \frac{f}{h_2} &= G_2[H + \gamma_2\gamma_3^{-1}(h_1 + h_2)] \\ \frac{f}{h_3} &= G_3(H) \end{aligned}\right\} , \qquad (2.28\text{a, b})$$

where G_2 and G_3 are arbitrary functions of their arguments. Now on $y = y_1$, for all trajectories emanating from the left of x_* in layer 3, $h_3 = (f_1/f_2)H$ by (2.16a) where $f_1 = f(y_1)$. Thus

$$G_3(H) = \frac{f_2}{H} = \frac{f}{h_3} \tag{2.29}$$

for those trajectories. Similarly in layer 2 in L all trajectories emanate from the northern region to the left of x_* so that on $y = y_1$, $h_2 = (1 - f_1/f_2)H$ and

$$H + \frac{\gamma_2}{\gamma_3}(h_1 + h_2) = H\left[1 + \frac{\gamma_2}{\gamma_3}(1 - f_1/f_2)\right], \quad y = y_1,$$

so that it is straightforward to see that

$$G_2\left[H + \frac{\gamma_2}{\gamma_3}(h_1 + h_2)\right] = \frac{f_1}{(1 - f_1/f_2)}\left[\frac{1 + \gamma_2\gamma_3^{-1}(1 - f_1/f_2)}{H + \gamma_2\gamma_3^{-1}(h_1 + h_2)}\right]. \tag{2.30}$$

Thus (2.29) and (2.30) imply that in region L

$$\left.\begin{aligned} h_3 &= (f/f_2)H\,, \\ h_2 &= \frac{f}{f_1}\left[\frac{1 + \gamma_2\gamma_3^{-1}(1 - f/f_2)}{1 + \gamma_2\gamma_3^{-1}(1 - f_1/f_2)}\right]\left(1 - \frac{f_1}{f_2}\right)H \\ h_1 &= \left\{1 - \frac{f}{f_2} - \frac{f}{f_1}\left[\frac{1 + \gamma_2\gamma_3^{-1}(1 - f/f_2)}{1 + \gamma_2\gamma_3^{-1}(1 - f_1/f_2)}\right] \times \left(1 - \frac{f_1}{f_2}\right)\right\}H. \end{aligned}\right\}, \tag{2.31a, b, c}$$

Again, the ratios of the layer thicknesses (h_1/h_2, h_1/h_3) are independent of the forcing, but now they do depend on the density differences between the layers.

The Sverdrup relation (2.5) can be written as

$$\frac{\partial}{\partial x}\left(H^2 + \frac{\gamma_2}{\gamma_3}(h_1 + h_2)^2 + \frac{\gamma_1}{\gamma_3}h_1^2\right) = \frac{\partial}{\partial x}D_0^2, \tag{2.32}$$

which with (2.31) may be rewritten entirely in terms of H to yield

$$H = [(D_0^2(x, y) + H_0^2)/F(y)]^{1/2}, \tag{2.33a}$$

where

$$F(y) = 1 + \frac{\gamma_2}{\gamma_3}\left(1 - \frac{f}{f_2}\right)^2 + \frac{\gamma_1}{\gamma_3}\left\{1 - \frac{f}{f_2} - \frac{f}{f_1}\left(1 - \frac{f_1}{f_2}\right)\left[\frac{1 + \gamma_2\gamma_3^{-1}(1 - f/f_2)}{1 + \gamma_2\gamma_3^{-1}(1 - f_1/f_2)}\right]\right\}^2. \tag{2.33b}$$

The potential vorticity trajectory $\tilde{x}_3(y)$ in layer 3 which emanates from x_* is given by

$$D_0^2(\tilde{x}_3, y) = (F(y) - 1)H_0^2, \tag{2.34}$$

and the resulting equation for $\tilde{x}_3(y)$ determines the boundary of L in layer 3 *and* layer 2.

We now examine the flow in region R. In this region layer 3 is stagnant, layer 1 is forced directly by the wind while potential vorticity is conserved in layer 2, i.e., as in (2.28a)

$$\frac{f}{h_2} = G_2\left[H + \frac{\gamma_2}{\gamma_3}(h_1 + h_2)\right].$$

However, $H = H_0$ within R and on *all* trajectories in layer 2 which enter at y_1. It then follows that

$$G_2[H + \gamma_2\gamma_3^{-1}(h_1 + h_2)] = G_2^*(h_1 + h_2) \tag{2.35}$$

where G_2^* is another arbitrary function. Evaluating G_2^* on y_1 where h_1 vanishes implies that

$$\frac{f}{h_2} = \frac{f_1}{(h_1 + h_2)} \tag{2.36}$$

or

$$\left.\begin{aligned} h_2 &= \frac{f}{f_1}(h_1 + h_2) \\ h_1 &= (1 - f/f_1)(h_1 + h_2) \end{aligned}\right\}, \tag{2.37a, b}$$

while the Sverdrup relation implies that

$$(h_1 + h_2) = (\gamma_3\gamma_2^{-1})^{1/2}\frac{D_0(x, y)}{[1 + \gamma_1\gamma_2^{-1}(1 - f/f_1)^2]^{1/2}}, \tag{2.38}$$

while of course

$$h_3 = H_0 - (h_1 + h_2). \tag{2.39}$$

Note the similarity between (2.38) and (2.20). However, now $h_1 + h_2$ must vanish on $y = y_1$ at $x = x_E$ so that the constant of integration must vanish. Again only h_3 can be non-zero at $x = x_E$ in our model.

The *western* boundary of region R is defined by the potential vorticity trajectory in layer 2 that emanates from x_*. This contour is a line along which, by (2.36), $(h_1 + h_2)$ is constant and equal to its value at x_*, namely $(1 - f_1/f_2)H_0$, so that the trajectory $\tilde{x}_2(y)$ satisfies

$$D_0^2(\tilde{x}_2, y) = \frac{\gamma_2}{\gamma_3}\left(1 - \frac{f_1}{f_2}\right)^2 \times H_0^2\left[1 + \frac{\gamma_1}{\gamma_2}(1 - f/f_1)^2\right]. \tag{2.40}$$

The trajectory $\tilde{x}_2(y)$ defines the eastern boundary of region M while $\tilde{x}_3(y)$ defines its western boundary. Within region M, layer 3 is at rest so that $H = H_0$. Potential-vorticity is conserved in layer 2 so that again

$$\frac{f}{h_2} = G_2\left[H + \frac{\gamma_2}{\gamma_3}(h_1 + h_2)\right]. \tag{2.41}$$

However, in contrast to region R, potential vorticity trajectories in layer 2 sweep across $y = y_1$ from the region to the left of x_* along which H is not a constant. As in region L, on $y = y_1$

$$h_2 = (1 - f_1/f_2)H,$$

so that (2.41) becomes

$$\frac{f}{h_2} = \frac{f_1}{(1 - f_1/f_2)}\left[\frac{1 + \gamma_2\gamma_3^{-1}(1 - f_1/f_2)}{H + \gamma_2\gamma_3^{-1}(h_1 + h_2)}\right], \quad (2.42)$$

or in terms of $(h_1 + h_2)$,

$$\left.\begin{aligned} h_2 &= \frac{f}{f_1}\left[H_0 + \frac{\gamma_2}{\gamma_3}(h_1 + h_2)\right]\frac{(1 - f_1/f_2)}{[1 + \gamma_2\gamma_3^{-1}(1 - f_1/f_2)]} \\ h_1 &= (h_1 + h_2)\left\{1 - \frac{f}{f_1}\frac{\gamma_2}{\gamma_3}\frac{(1 - f_1/f_2)}{[1 + \gamma_2\gamma_3^{-1}(1 - f_1/f_2)]}\right\} - H_0\frac{f}{f_1}\frac{(1 - f_1/f_2)}{[1 + \gamma_2\gamma_3^{-1}(1 - f_1/f_2)]} \end{aligned}\right\}, \quad (2.43\text{a, b})$$

while the Sverdrup solution yields a quadratic equation for $h_1 + h_2$ whose solution is

$$h_1 + h_2 = \left\{\frac{\gamma_1}{\gamma_2}ab + \left[\frac{\gamma_3}{\gamma_2}D_0^2\left(1 + \frac{\gamma_1}{\gamma_2}a^2\right) - \frac{\gamma_1}{\gamma_2}b^2\right]^{1/2}\right\} \times \left(1 + \frac{\gamma_1}{\gamma_2}a^2\right)^{-1}, \quad (2.44)$$

where

$$\left.\begin{aligned} a &= \left\{1 - \frac{f}{f_1}\frac{\gamma_2}{\gamma_3}\left[\frac{(1 - f_1/f_2)}{1 + \gamma_2\gamma_3^{-1}(1 - f_1/f_2)}\right]\right\} \\ b &= H_0(f/f_1)(1 - f_1/f_2)/[1 + \gamma_2\gamma_3^{-1}(1 - f_1/f_2)] \end{aligned}\right\}.$$

This completes the solution in the hybrid region M. It is straightforward, but algebraically tedious, to demonstrate that the solutions for h_1, h_2 and h_3 in L, M and R are continuous across their common boundaries, i.e., along $\tilde{x}_2$ and $\tilde{x}_3$ as defined by (2.21) and (2.26).

Although the solution has split into three parts, the major qualitative differences occur in crossing $\tilde{x}_3(y)$ between L and M. The latter region shares with R a stagnant layer 3. The trajectory $\tilde{x}_3$ rapidly slices westward for most realistic distributions of w_e (i.e., D_0^2). Since D_0^2 goes to zero as the equator is approached [as long as $(w_e f)$ remains finite] it follows that $\tilde{x}_3(y)$ must strike the western boundary at some point north of the equator. In our model, the bottom of the lowest layer of the subtropical thermocline system must become flat upon entering low latitudes, i.e., south of $\tilde{x}_3(y)$.

To the east of $\tilde{x}_3(y)$ the total Sverdrup transport must be carried by the upper layers alone while west of $\tilde{x}_3(y)$ the transport is partially carried by layer 3. This in turn implies that the upper layers will have generally steeper horizontal gradients east of $\tilde{x}_3(y)$.

The solution west of $\tilde{x}_3(y)$ may also bifurcate into separate zones. In distinction to the solution splitting in the eastern ocean the existence of a western solution splitting depends in a sensitive way on the positions of y_1 and y_2 with respect to the maximum (or maxima) of D_0^2. If D_0^2 increases equatorward in some latitude band, potential vorticity trajectories will tend to curve eastward as they thread southward to preserve H and hence potential vorticity. This implies that some zones with a large enough H as given by (2.20) cannot be matched along a potential-vorticity contour to an image point along y_2. To be more precise, we must consider whether any potential vorticity trajectory emanating from $y = y_2$ grazes the western boundary and then turns eastward. If so, a region southwestward of this trajectory will be denied access to $y = y_2$ and must remain unventilated. Within layer 3 the potential vorticity trajectories which emerge from y_2 are coincident with lines of constant H.

The critical trajectory, if it exists, will have $\partial x/\partial y)_H = 0$ on $x = x_w$, $y = y_*$, and will have $\partial x/\partial y)_H < 0$ south of y_*. Now

$$\left.\frac{\partial x}{\partial y}\right)_H = -\frac{\partial H/\partial y}{\partial H/\partial x} = -\frac{\partial H^2/\partial y}{\partial H^2/\partial x}. \quad (2.45)$$

Since, by (2.20),

$$\frac{\partial H^2}{\partial x} = \frac{\partial D_0^2}{\partial x}\left[1 + \frac{\gamma_2}{\gamma_3}(1 - f/f_1)^2\right]^{-1} < 0 \quad (2.46)$$

as long as $w_e < 0$, $\partial x/\partial y)_H$ has the same sign as $\partial H/\partial y$. In order for $\partial H/\partial y \leqslant 0$ we must have, on $x = x_w$,

$$\frac{\partial D_0^2}{\partial y} \leqslant -2\frac{\gamma_2}{\gamma_3}\frac{\beta}{f_2}\frac{(1 - f/f_2)(D_0^2 + H_0^2)}{[1 + \gamma_2\gamma_3^{-1}(1 - f/f_2)^2]}, \quad (2.47)$$

where, recall,

$$D_0^2 = \frac{-2f^2}{\beta\gamma_3}\int_x^{x_E} w_e(x', y)dx'.$$

At the point y_*, Eq. (2.47) becomes an equality and a potential vorticity trajectory will emerge from (x_w, y_*), encompassing a region impenetrable to ventilating streamlines. In general $\partial D_0^2(y_*)/\partial y$ must be negative for a y_* to be realized. A particularly interesting case occurs when y_* is coincident with y_2. In this case $\partial x/\partial y)_H$ need not be zero at x_w. All that is required is that $\partial x/\partial y)_H$ be negative on $y = y_2$. From (2.47) this merely requires that $\partial D_0^2/\partial y < 0$ on $y = y_2$, $x = x_w$. Since D_0^2 is generally an increasing function of y for small y and is a decreasing function of y near $y = y_w$ (where w_e vanishes), the condition

$\partial D_0^2/\partial y < 0$ at $y = y_2$, $x = x_w$, requires that D_0^2 achieve its maximum south of y_2. In this case the equation for the separating trajectory x_s emanating from (x_w, y_2) is

$$D_0^2(x_s, y) = D_0^2(x_w, y_2)\left[1 + \frac{\gamma_2}{\gamma_3}(1 - f/f_2)^2\right] + H_0^2 \frac{\gamma_2}{\gamma_3}(1 - f/f_2)^2. \quad (2.48)$$

In the vicinity of y_2, D_0^2 need only increase southward for x_3 to thread eastward. As y departs from y_2 the terms in $(1 - f/f_2)^2$ on the right-hand side of (2.48) will tend to direct x_s westward until x_s again strikes x_w enclosing an isolated unventilated region at the western edge of the ocean. The larger H_0 is, the smaller this region will be, but as long as $\partial D_0^2/\partial y < 0$ at y_2 some finite closed region will occur as shown in Fig. 3.

Within this region (2.14) no longer applies and we have no *a priori* prescription for the specification of $G_2(H)$ on any contour emanating from x_w and returning to it. One possibility is to identify this region with the constant potential vorticity pool in the model of Rhines and Young (1981), although we hasten to add that the boundary of our region does not coincide with theirs since we have motion occurring exterior to the region in layer 3. If we attribute to this entire pool in layer 3 the constant potential–vorticity of its girdling trajectory x_s, then within the region

$$h_3 = \frac{f}{f_2} H(x_w, y_2) = \frac{f}{f_2}[D_0^2(x_w, y_2) + H_0^2]^{1/2}. \quad (2.49)$$

The Sverdrup relation (2.5) yields

$$(h_2 + h_3)^2 + \gamma_2\gamma_3^{-1}h_2^2 = D_0^2 + H_0^2,$$

which with (2.49) yields h_2, *viz*:

$$h_2 = -\frac{(f/f_2)[D_0^2(x_w, y_2) + H_0^2]^{1/2}}{(1 + \gamma_2\gamma_3^{-1})} + \frac{1}{(1 + \gamma_2\gamma_3^{-1})}\left\{[D_0^2(x, y) + H_0^2](1 + \gamma_2\gamma_3^{-1}) - \frac{\gamma_2}{\gamma_3}\frac{f^2}{f_2^2}[D_0^2(x_w, y_2) + H_0^2]\right\}^{1/2}. \quad (2.50)$$

Again, it is a simple matter to show that on x_s, h_2 and h_3 are continuous and the ventilated and unventilated regions match smoothly.

In principle $x_s(y)$ could intersect y_1 before it reattaches at x_w. In that case the region of uniform potential vorticity in layer 3 must be matched to the external ventilated flow through a buffer region in a manner similar to the matching that occurs to the stagnant region on the eastern boundary. The more elaborate calculation required is straightforward although algebraically tedious, and will not be repeated here.

The final region requiring discussion is the region $y > y_w$. Here w_e is positive (upwelling) so that the function D_0^2 is always negative. Nevertheless (2.9) is still valid in this region as long as $D_0^2(x, y) + H_0^2 > 0$. On the line $y_3(x)$ defined by

$$\int_x^{x_E} w_e(x', y_3(x))dx' = \frac{\beta\gamma_3}{2f^2}H_0^2, \quad (2.51)$$

the interface between layers 3 and 4 rises to the surface. Since both w_e and $\partial w_e/\partial y > 0$ in this region, the intersection line $y_3(x)$ will generally slope southwest to northeast (Fig. 3). Since

$$\nabla h_3 = \frac{\nabla D_0^2}{(D_0^2 + H_0^2)^{1/2}} = \frac{\nabla D_0^2}{h_3}, \quad (2.52)$$

the interface at the surface slopes upward, vertically yielding a singularity in the geostrophic velocity at y_3 but of course a finite transport here. Recall that south of y_w layer 4 is entirely at rest. This stagnant condition of layer 4 will be maintained south of $y_3(x)$ and its lower surface (the interface between layer 4 and layer 5) will be utterly flat. North of $y_3(x)$ layer 4 is directly exposed to the Ekman upwelling so that north of $y_3(x)$

$$h_4^2 = -\frac{2f^2}{\beta\gamma_4}\int_x^{y_3^{-1}(x)} w_e dx' + H_4^2, \quad (2.53)$$

where $\gamma_4 = g(\rho_5 - \rho_4)/\rho_0$ and $y_3^{-1}(x)$ is the longitude of the surfaced position of h_3. The constant H_4 is the depth of the interface between layers 4 and 5 in the region south of $y_3(x)$. Of course h_4 will be rising to the surface as y increases, and depending on the extent of the subpolar region and the initial depths of the deeper layers, one isopycnal after another can be pulled to the surface by the Ekman upwelling along lines $y_j(x)$, $j > 3$. These intersection lines in the upwelling region cannot be prescribed *a priori*. Fluid is leaving, rather than entering, the domain of flow and neither density nor potential vorticity can be prescribed on the upper surface.

In the solution we have prescribed here for the subpolar gyre only the uppermost layer, driven directly by the wind stress, is in motion. Although this is in one sense the simplest possible solution consistent with Sverdrup dynamics it is not unique. Since fluid is entering the interior from the region of the western-boundary-current system we may, in principle, set each of the layers below layer 3 into motion by specifying a non-zero zonal inflow at $x = x_w$, i.e., by redistributing the zonal Sverdrup transport over the depth. For all the shielded layers this would specify as well the potential vorticity of the fluid entering the region and the resulting flow could then be calculated in the same manner as the multi-layered flow in the subtropical gyre. However, a little thought shows that the technical difficulties in actually carrying through such a calculation are non-trivial and there are, in addition, considerable uncertainties as to the appropriate latitudinal distribution of the entering flow. We therefore reserve such a calculation for future study.

Nevertheless, we wish to point out this possible extension of the theory for the subpolar gyre now for two reasons. First of all, it becomes immediately clear that there is no intrinsic reason why the subpolar circulation will be limited to the upper layer. Sources of flow in the subpolar gyre that may arise along the perimeter of the Sverdrup interior will drive lower-layer motions. Second, discrepancies between the model's predictions and the observed ocean in the subpolar gyre may be due to deficiencies in the particular solution we present (which has no deep western inflow specified) rather than due to a fundamental physical deficiency in the model's applicability to the subpolar gyre.

3. General remarks

In the following section a particular, and we think, fairly realistic example is discussed that will make clearer the points raised during the preceding analysis. It is useful, though, first to describe certain salient qualitative features of the general problem and its solution.

One of the most important and obvious results is the strong dependence of the solution on the *local* value of D_0. The position of the base of the moving region and the individual layer thicknesses are each an increasing function of D_0 within the ventilated region. Now D_0^2 involves an integral of the Ekman pumping from the general point (x, y) to the eastern boundary at the same latitude. Information and the influence of distant wind-stress curl propagates westward in latitude strips each one of which is essentially independent of neighboring latitude bands. Increased Ekman pumping at higher latitudes does not deepen the thermocline or make more vigorous the circulation at latitudes south of such a zone of enhanced downwelling. As (2.21a) shows, increasing the downwelling at the latitude of outcropping will only alter the trajectory of the flow, causing the fluid to move more sharply westward if D_0 is held fixed south of the outcrop. The Eulerian solution is local in its latitude dependence. It is interesting to note that one nonlocal feature of the solution (as far as *latitude* dependence is concerned) is the solution's memory of the latitude of outcrop of each isopycnal layer. As (2.16a,b) and (2.31a,b,c) demonstrate, the ratio of layer depths at any latitude in the ventilated zone is a function of only the distance from the outcrop and the density differences between the layers.

An important exception to the local dependence on wind-stress curl is the size of the western unventilated region which we have identified as a zone of constant potential vorticity. In this case (2.48) demonstrates that the Ekman pumping increasing the downwelling at the outcrop will tend, all else held equal, to reduce everywhere the extent of the unventilated zone.

The thickness of layer 3 at the latitude of vanishing wind-stress curl is the constant H_0. Therefore there is no geostrophic flow across this latitude, i.e., no geostrophic communication between the subpolar and subtropical gyres. By continuity this layer depth is equal to H_0 along the eastern boundary and this important parameter of the solution plays an important role in determining the magnitude and geometry of both the eastern and western unventilated zones. The eastern shadow region increases with H_0 while the western zone decreases if H_0 is increased. Another very important role H_0 plays is its moderating influence on the longitudinal variation of the potential vorticity of the fluid along its subducting latitude. For example at the first subduction latitude the potential vorticity of layer 3 is

$$\frac{f}{h_3} = \frac{f_2}{H} = \frac{f_2}{(D_0^2 + H_0^2)^{1/2}}, \quad y = y_2. \tag{3.1}$$

For a fixed $D_0(x, y)$ the effect of increasing H_0 is to reduce the range of variation of the potential vorticity along the outcrop zone. Since this potential vorticity is then carried into the ventilated zone south of y_2, an increase of H_0 will tend to produce a zone of relatively weak (though dynamically vital) potential vorticity variation within the fluid. This is especially vivid in the example discussed in the following section. H_0 also increases the latitude of density outcropping in the subpolar gyre.

An important technical simplification in our solution occurs because we have chosen the position of the density outcrops to be coincident with latitude circles. Again, by continuity and the eastern boundary condition, these layers must have vanishing depth along the eastern boundary. As a consequence the potential vorticity of the upper moving layers rapidly increases as the eastern boundary is approached. This in turn implies that the separating trajectory $\tilde{x}_3(y)$ emanating from the eastern boundary also tends to divide regions of weak and strong potential vorticity gradient.

We have emphasized repeatedly the fact that the thermocline structure we have deduced from our model is decidedly non-self-similar. The relative velocities and transports between the layers depends in a gross way on the region of the flow. In particular, the increasing foliation of regions with an increase in the number of layers in the western and eastern shadow regions leads to great complexity in the analytical structure of the solution. In view of this it is useful to recall that a form of *local* similarity does survive within the ventilated region where, as noted earlier, the ratio of layer thicknesses depends only on the distance from the outcrop latitude. It is important to note that this similarity may be peculiar to the case where the density outcrops in the subtropical gyre are along latitude circles. Preliminary calculations show that in the more general case the inversion of (2.14) will retain a dependence on the Ekman pumping at the outcrop. Further study will be required to illuminate this rather complex dependence. We note that even this weak trace of self-similarity in the case we have calculated fails within the two shadow regions.

The overall geography of the thermocline is easily described. In the subtropical gyre the overall depth of the thermocline (H) increases westward, except in the zone east of $\tilde{x}_3(y)$ where it is constant. Because D_0^2 has a maximum at some latitude between the equator and y_w, H deepens south of y_w and then gradually rises to a constant value H_0 at a southern latitude determined by the separation trajectory $\tilde{x}_3(y)$. The upper two moving layers also achieve local maxima in depth at middle latitude and each of them rises to the surface at the equator in a manner consistent with potential vorticity conservation. It is important to note that this rise to the surface does not imply equatorial upwelling. The total depth of the region of moving fluid simply shrinks as the equator is approached. In this equatorial zone south of the $\tilde{x}_3(y)$ trajectory the upper of the two moving layers is the thicker and carries most of the geostrophic transport. In the region of the subtropical gyre north of the separating trajectory it is always the surface layer which occupies an increasing fraction of the total depth as the fluid moves southward.

In our discussion we have assumed that x_w represented the western boundary of the oceanic Sverdrup regime. We are supposing that an as yet undetermined western-boundary-current region can be joined to this Sverdrup interior. This is one of the model's critical deficiencies shared by all Sverdrupian thermocline models. We have no *a priori* theoretical justification to suppose that a western dynamical region exists which is compatible in every way with the interior solution we have found. Indeed, observations and previous theoretical work suggest that the zone of influence of the higher order dynamics of the western ocean may significantly penetrate eastward, contaminating a fair portion of the solution we present here. It is therefore important to emphasize that the interior region east of this zone of influence will remain as calculated in this model. This is true simply because within the Sverdrup region information is propagated westward. Western dynamics may slice off portions of our picture but should leave the remainder unchanged.

The second deficiency of our model is the absence of explicit eddy processes. We have not discussed the stability properties of our model but it should be clear that the condition that isopleths of potential vorticity depart significantly from latitude circles is equivalent to remarking that the necessary conditions for baroclinic instability are likely to be satisfied. The consequences of the resulting eddy activity on the structure of our thermocline are not known.

In the subtropical gyre where layer 4 is at rest, the layer will possess an ambient potential vorticity $f/h_4 = f/(H_4 - H)$, where H_4 is the constant depth of the base of layer 4. The associated potential-vorticity gradient is

$$\nabla \frac{f}{h_4} = h_4^{-2}\left[\mathbf{i}f\frac{\partial H}{\partial x} + \mathbf{j}\left(\beta h_4 + f\frac{\partial H}{\partial y}\right)\right]. \tag{3.2}$$

If we consider latitude regions where $w_e < 0$ for all x then f/h_4 can never have an interior maximum. However H increases monotonically from x_E westward to x_w so that if $\partial H/\partial y = -(\beta/f)h_4$ for some $y = \hat{y}$ on $x = x_w$ a maximum will occur on the boundary. This point $(x_w, \hat{y})$ will then be the center of lines of constant ambient potential vorticity in layer 4 and we suggest that it may be in this subthermocline, unventilated zone that the homogenization of potential vorticity suggested by Rhines and Young (1981) will occur.

Finally, another important feature of the model we wish to bring out is that, although the fluid over a large part of the flow is ventilated, this does not imply that water columns moving through the outcropping region are completely volumetrically renewed with water from the mixed layer. This fact is obscured by Stommel (1979). This is especially important if inferences about tracer distributions are to be drawn from the model for comparison with oceanic observation. To demonstrate the incompleteness of volume renewal consider the motion of fluid columns in the region $y_2 < y < y_w$, where layer 3 is directly exposed to Ekman pumping. In general a fluid column will move eastward and southward along a line of constant $h_3 = H$ absorbing water pumped downward from the Ekman layer. For a fluid column initially at $x = x_w$, $y = y_N \leq y_w$ which then travels on a broad clockwise arc to some point (x, y_2) where it is subducted below layer 2, the volume of water absorbed from the Ekman layer per unit area of the column is

$$\Delta z = -\int_0^t w_e(x, y)dt, \tag{3.3}$$

where t is the time required to traverse the arc described above. Now

$$dt = \frac{dy}{v_3},$$

while from (2.11),

$$v_3 = \frac{f}{\beta h_3} w_e.$$

Hence (3.3) may be written

$$\Delta z = -\int_{y_N}^{y_2} h_3 \frac{\beta}{f} dy, \tag{3.4}$$

where the integration is along the streamline of flow. Since h_3 is a constant on geostrophic streamlines in this region

$$\frac{\Delta z}{h_3} = \ln[f(y_N)/f(y_2)]. \tag{3.5}$$

Of course each clockwise contour has a different y_N. Those with larger y_N will sweep farther eastward so that the volume fraction of the column added by Ekman pumping should generally increase *eastward* along y_2 (or, in fact, along any latitude). For most reasonable values of y_N and y_2, $\Delta z/h_3 < 1$ so that the fraction of layer 3 directly renewed is less than 1. However, since the new water is pumped into subsurface water of the same density, in actuality we can expect any tracer to be distributed down from the mixed layer into the entire water column of the ventilated layer. The mass of that ventilated water circulating horizontally is considerably greater than the mass added from the mixed layer.

4. Application to the thermocline in the North Atlantic Ocean

In this section we will show that the model predicts an unventilated region sweeping across the entire low-latitude North Atlantic from the eastern boundary at the depth of the 27.40 isopycnal surface. The observed distributions of dissolved oxygen and tritium on this surface are indicative of poor ventilation.

There are large regions of nearly uniform potential vorticity, in which small variations control the flow.

To apply this model to the North Atlantic we choose a three-layer representation of the thermocline; a fourth bottom layer is assumed to be at rest, and the interface between layers 3 and 4 is then taken to be the upper limit (in potential density) for the fluid pumped down into the subtropical gyre by the Ekman pumping. The other layers are chosen to represent densities that intersect the sea surface in the wintertime, within the interior of the subtropical gyre.

The particular choice of isopycnal layers is arbitrary—we have chosen the potential density values given in Table 1. The interfaces between the layers are at σ_θ = 27.40, 27.00, 26.20. The relative density differences γ which are used in the thermal wind relations are found by using the mean density in each layer.

The surface density in the North Atlantic is a strong function of the season. One would expect, as argued by Stommel (1979), that the density of the fluid that escapes (is subducted) is set by the density of the mixed layer when it is deepest, in the wintertime. Thus we expect that the density and latitude at subduction will be determined by the wintertime surface density distribution. For this simple model calculation, we assume that these subduction zones are circles of latitude, so that we take the zonally averaged latitude from Böhnecke (1936). These latitudes are given in Table 2. Wintertime outcropping of densities $\geq$ 27.40 occur to the north of the northern boundary of the subtropical gyre, the zero of the Ekman pumping.

In addition to the specific choices of isopycnal surfaces and subduction latitudes, we must specify the depths of these surfaces along the eastern boundary of the model. The 27.40 isopycnal can be seen from the IGY sections (Fuglister, 1960) shown in Fig. 4 to intersect the eastern boundary at a nearly constant depth, ranging from 800 m at 48°N to 950 m at 16°N; for this calculation we take a constant value of 800 m. Choosing a depth at the eastern wall that varies with latitude would imply a mass flux normal to the eastern wall—a situation that we have chosen not to allow.

The shallower interfaces corresponding to σ_θ = 26.20, 27.00, also shown in Fig. 4 from the IGY sections, actually have variable depth along the eastern boundary from 0–300 m. To avoid a mass flux normal to the eastern wall, we choose their limiting values to vanish there. Within the confines of our model any layer that outcrops within the subtropical gyre (i.e., that region where $w_e < 0$) must vanish along the eastern wall. It is interesting to note that if a layer has a prescribed (constant) non-vanishing depth along the eastern wall, none of the layers beneath it can be forced into motion by this mechanism in the subtropical gyre—there can be only one layer which

TABLE 1. Density parameters of the three-layer model.

Layer	Mean σ_θ	Range of σ_θ	$\gamma = \frac{\Delta\rho}{\rho_0} \times 10^3$
1	25.70	25.20–26.20	0.9
2	26.60	26.20–27.00	0.6
3	27.20	27.00–27.40	0.55
4	27.75		

TABLE 2. Latitudes where layer interfaces reach surface in winter.

σ_θ	Range of latitude (°N)	Zonal mean latitude (°N)
26.20	32–18	25
27.00	40–35	37.5
27.40	55–48	51.5

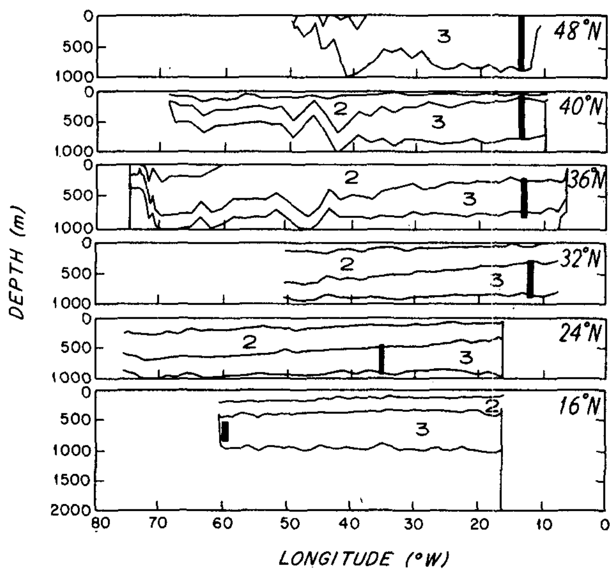

FIG. 4. Isopycnal surfaces from IGY sections (Fuglister, 1960). The isopycnals are 26.20, 27.00 and 27.40. The thick stripe in each section corresponds to the location of a fluid column of an arbitrary but fixed potential vorticity. See text for details.

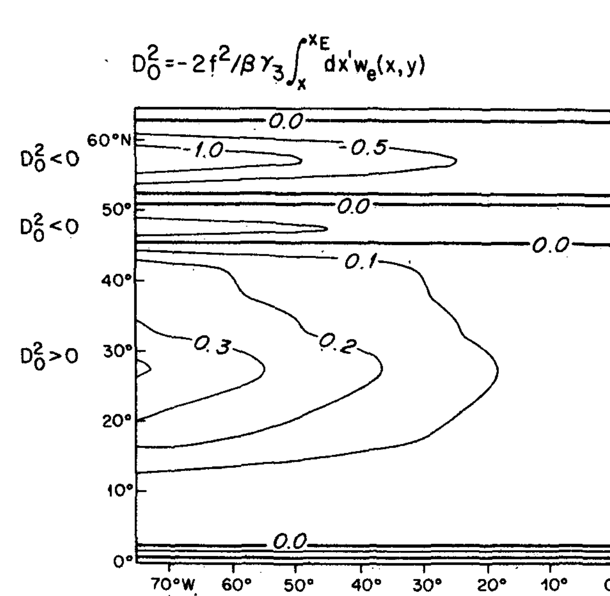

FIG. 5. Contour plot of the Sverdrup function in units of km².

is in motion in both the subtropical ($w_e < 0$) and subpolar ($w_e > 0$) gyres.

It remains to prescribe the vertical flux at the base of the Ekman layer. This flux has been computed by Stommel (1964), Leetmaa and Bunker (1978) and others. Arguing in a manner similar to that for using the wintertime surface density, the total amount of fluid pumped down from the Ekman layer is determined by the annual mean Ekman flux. As with the subduction lines, we use the zonally averaged Ekman flux, linearly interpolated between the 5° squares, given by Stommel (1964). The resulting distribution of the Sverdrup function D_0^2 (in 10^3 m) is shown in Fig. 5.

As we discussed in Part I, the potential vorticity in each layer is conserved once that layer has been subducted. The range of potential vorticities available to the fluid in a particular layer is determined by the potential vorticity distribution along the line of subduction. For layer 3, the maximum and minimum values are found at the extreme eastern and western edges of the region. The trajectories emanating from those extreme values delineate distinct regions of flow—a stagnant region along the eastern edge and a constant potential vorticity region to the west. When the second layer becomes subducted, there are trajectories in layer 2, emanating from the boundaries between the regions in layer 3, that do not in general coincide with the trajectories in layer 3. These various trajectories are shown in Fig. 6, a plan view illustrating the geometry of the model, the subduction latitudes and the regions of flow.

For simplicity, we have chosen a rectangular domain for the computations. The inclusion of the African landmass is straightforward, but changes the detail flow patterns, although not in an essential manner.

The layer depths for each of the three active layers are presented as contour plots in Fig. 7. The feature which is most clear from these plots is the large region of uniform depth in layer 3 sweeping across from the subduction point on the eastern wall to the western boundary of the calculations in which there is no motion. The boundary between the region of no flow and flow in layer 3 is the potential vorticity trajectory, shown in Fig. 6, emanating from the eastern boundary. When this trajectory intersects the subduction latitude for layer 2 (y_2 = 25°N), a second dividing potential vorticity trajectory separates the flow in

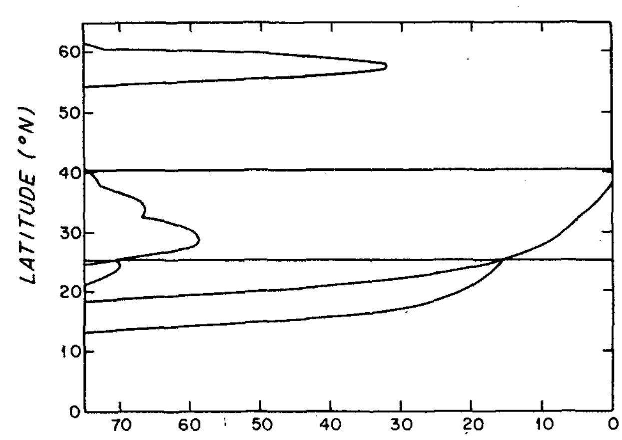

FIG. 6. Plan view of the model basin showing the trajectories of potential vorticity.

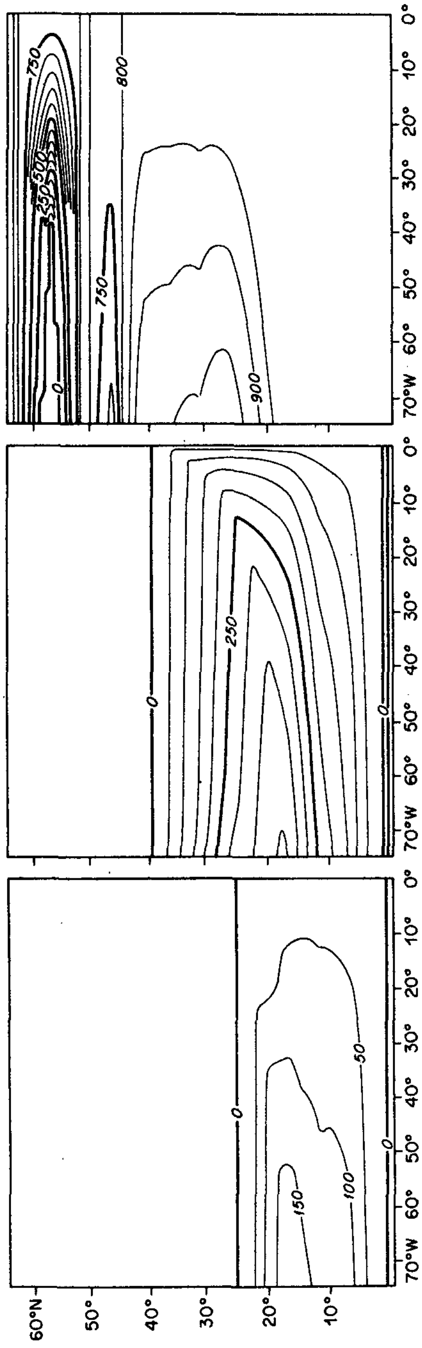

FIG. 7. Contour plots of the lower interfaces for each of the three active layers, the contour level is 0.05 km.

layer 2 into two regions—one overlying the ventilated region in layer 3 and the other overlying the unventilated region. This division is marked by a local change in the slope of the interfaces which we would not expect to distinguish in the presence of the natural variability in the ocean.

Since most available hydrographic data are in the form of sections, we show in Fig. 8 sections through the model along 30°W, 50°W, 30°N and 15°N. The general shape of the density interfaces corresponds to that shown in Fig. 4. Each of those who seek to make a detailed comparison of the model results with the observed density (and potential vorticity) field of the real North Atlantic will see through different eyes. One need not expect such an elementary model to replicate all features in all geographic regions of the ocean. The reasons are so manifold that it would be exceedingly tedious to try to discuss them all, and it would lay a burden on the reader out of proportion to the significance of the results obtained. Instead, we restrict ourselves to two of the most obvious reasons: land and high-energy eddies. Both are shown schematically on Fig. 9, upon which is also drawn the field of depth of the 27.4 σ_θ surface from the model. In rough terms, the area for valid comparison lies to the eastward of the heavy dashed curve and where there is no land. The dashed boundary has been located by comparison of the real density slopes and computed slopes at two longitudinal sections: (i) the IGY section at 50°W (Luyten and Stommel, 1982) and (ii) the central density section in Wüst's essay on the stratosphere of the Atlantic Ocean (Wüst, 1935).

On the 50°W section we note that the actual and computed slopes of the 27.4 surface differ in sign north of about 25°N. On the Wüst section this opposition in sign occurs at about 55°N in the center of the subpolar gyre. The dashed curve is fixed at these two critical points. In the former case the explanation of the contradictory signs probably lies in the existence of western-boundary currents, recirculation and energetic eddy processes, which the model does not include. In the latter case it may be due to deep wintertime convection and mixing. We refrain from making finer geographical distinctions in comparison of model and reality in the belief that the above will be sufficient warning.

The cornerstone of our model is the conservation of potential vorticity in those layers that are not in direct contact with the Ekman flux. Thus fluid columns in the ventilated region can be traced back to their subduction latitude by their potential vorticity; fluid columns in the unventilated region cannot. This procedure can be applied to the IGY sections as well. In Fig. 4, we have chosen a particular fluid column between isopycnals 27.00 and 27.40 (our layer 3) in the 48°N section, marked there by the heavy vertical stripe. The thickness of this column shrinks with decreasing latitude, conserving its potential vorticity. As

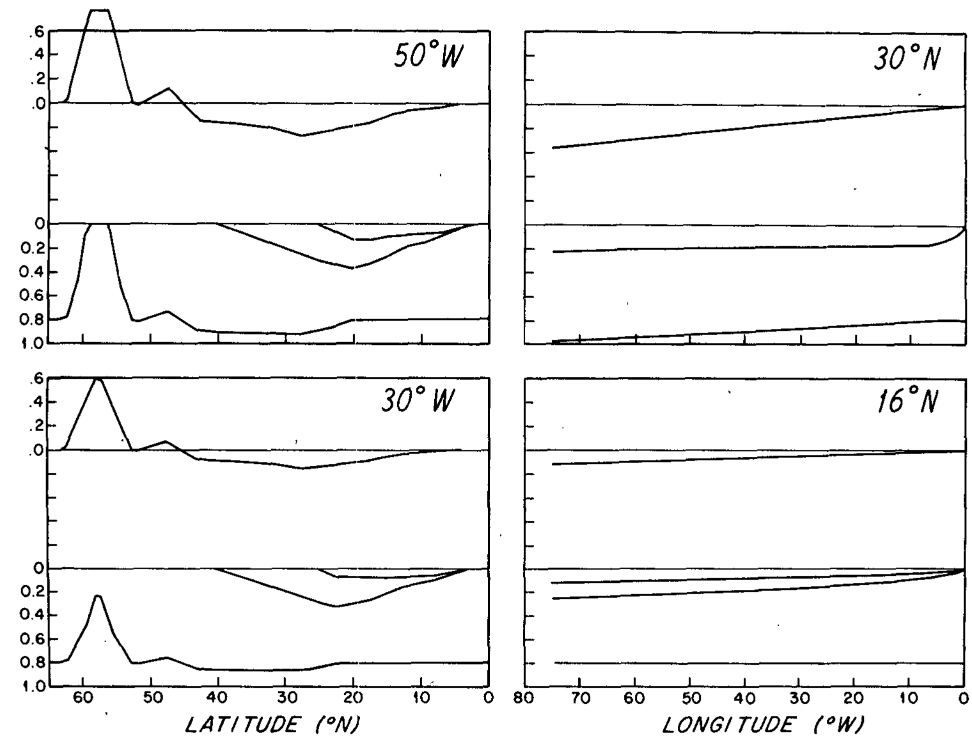

FIG. 8. Sections of layer depth (km) through the model at 50°W, 30°W, 30°N and 16°N. In each panel, the uppermost line is the Sverdrup function [sign(D_0)|D_0|], since $D_0^2 < 0$ in the subtropical gyre.

we progress to lower latitudes, the location of a fluid column of the same potential vorticity is marked on the sections at lower latitudes (32°N, 24°N), sweeping across the section from east to west. The 27.40 isopycnal is nearly flat to the east of this column of constant potential vorticity. By 16°N, the layer is everywhere too thick (potential vorticities too small) to trace back to the north and the 27.40 surface is flat across the entire section. This region of low potential vorticities that cannot be traced back to the subduction latitude, bounded below by a flat surface, has the characteristics of the unventilated region.

The distribution of dissolved oxygen provides some measure of the ventilation of fluid to the atmosphere. To compare with our layered model, we have taken the average content of dissolved oxygen as 27.00–27.40 between the isopycnal surfaces bounding our layer 3. The distribution of this quantity along each of the IGY meridional sections, shown in Fig. 10, illustrates the depletion in dissolved oxygen in layer 3, with decreasing latitude, particularly along the eastern flank of the ocean. This is consistent with our interpretation of this low potential vorticity region as unventilated. The observed distribution of dissolved

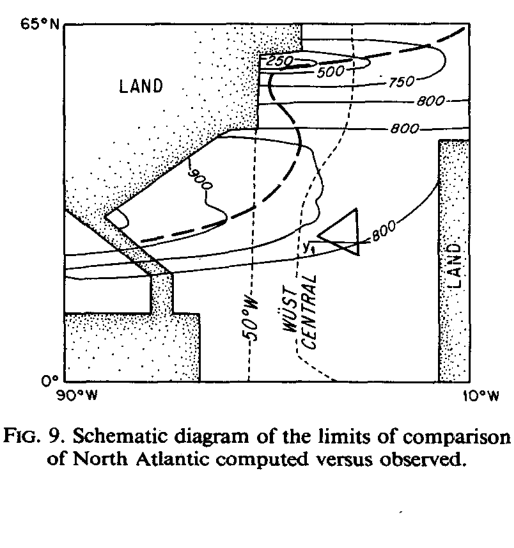

FIG. 9. Schematic diagram of the limits of comparison of North Atlantic computed versus observed.

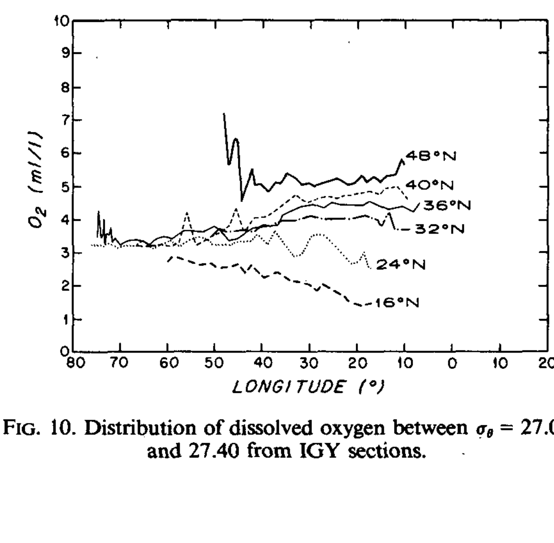

FIG. 10. Distribution of dissolved oxygen between σ_θ = 27.00 and 27.40 from IGY sections.

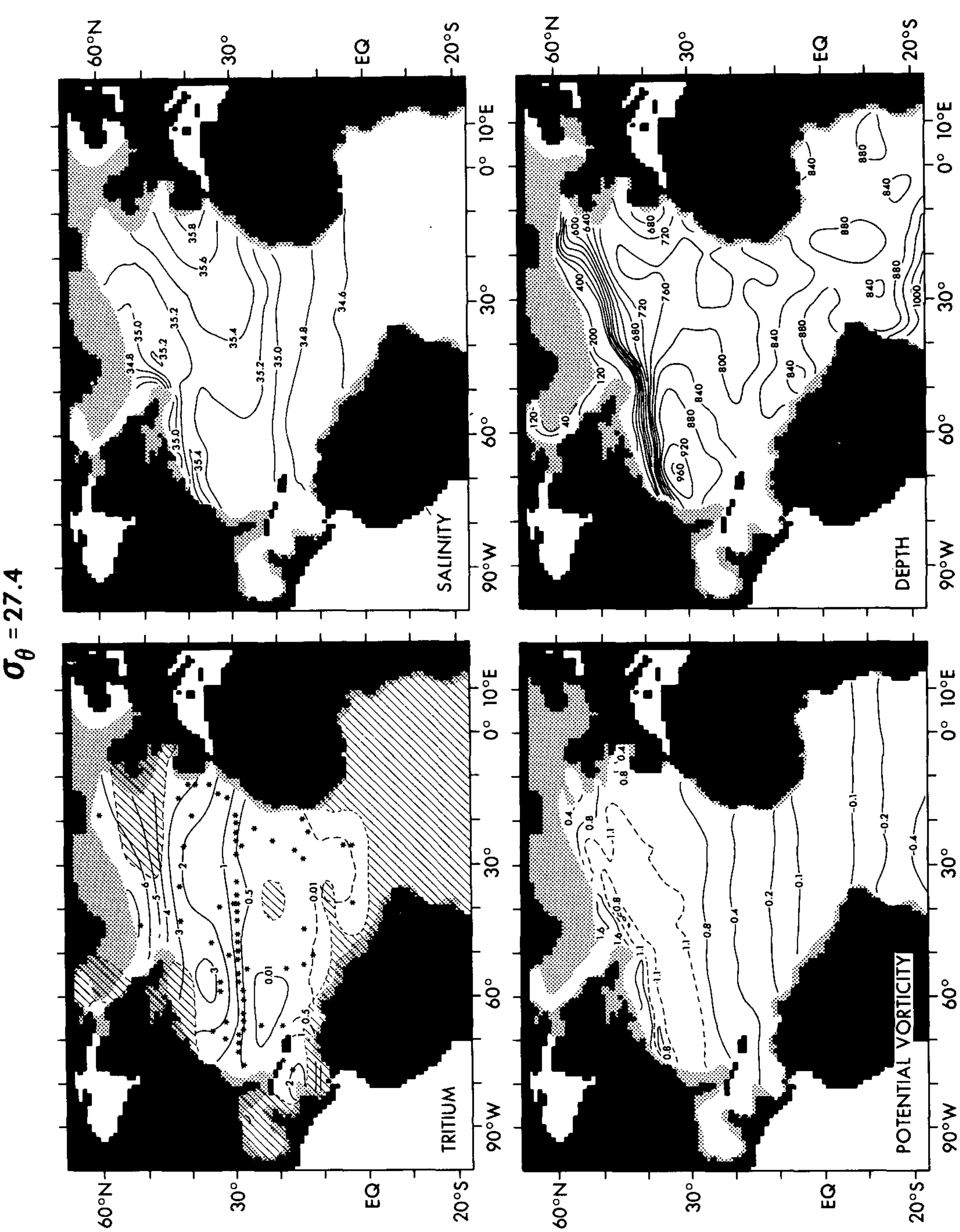

FIG. 11. Maps of tritium concentration (TU) and potential vorticity ($\times 10^{-5}$ s^{-1}) on isopycnal surfaces from Sarmiento *et al.* (1982).

oxygen must represent a balance between consumption by biological activity and processes of diffusion and advection which replenish the dissolved oxygen.

A classical interpretation of the oxygen minimum found near the eastern boundary was an increase in consumption due to upwelling along the eastern boundary, rather than a decrease in replenishment because of a lack of ventilation [see Menzel and Ryther (1968), particularly the last two pages].

A tracer which gives a more direct measure of ventilation is tritium. There are no sections of tritium that are comparable to the IGY data, but W. Jenkins (personal communication, 1981) has generously shown us a meridional section of tritium and oxygen along 38°W, which shows a dramatic reduction with decreasing latitude in tritium concentration for $\sigma_\theta > 27.0$. This result is consistent with the interpretation of this region as unventilated. Maps of tritium on particular isopycnal surfaces, prepared by J. Sarmiento [Sarmiento *et al.* (1982) and shown in Fig. 11] are generally consistent with our conjecture that there are at least two regions in the thermocline of the North Atlantic—one connected directly to northern latitudes where the fluid is ventilated to the atmosphere and forced downward by Ekman pumping, conserving potential vorticity after subduction, and another region which is not ventilated to the atmosphere.

A third region of the model flow was described above, in which the potential vorticity had a constant value. The existence of such a region was assumed in order to deal with regions of possibly closed geostrophic contours in which one could not *a priori* determine the potential vorticity. Our assumption was that these might be regions in which the vorticity homogenization discussed by Rhines and Young (1982) would apply. We cannot provide observational basis for the existence of such regions. Maps of potential vorticity also prepared by J. Sarmiento (and shown in Fig. 11) show large regions of the North Atlantic in which the potential vorticity is nearly uniform.

From our model we can compute potential vorticity in the lowest active layer as shown in Fig. 12. Throughout most of the ventilated region, as pointed out in section 3, the potential vorticity is nearly constant—in fact, most of the variation occurs in a small region. However, the variation in potential vorticity is dynamically important throughout the ventilated region. We suggest that the dynamically important gradients may be so small that they will be obscured by observational noise in the real ocean.

In layer 2, a similar situation occurs. Most of the variation in thickness of layer 2 occurs near the eastern boundary. Over most of the region where layer 2 has been subducted and must conserve potential vorticity, the potential vorticity is nearly constant although again its variations are dynamically important.

The results of the model suggest that the existence of large regions in the thermocline of the North Atlantic of nearly constant potential vorticity does not imply that these regions have *identically* constant potential vorticity—the dynamics may still be simple linear and Sverdrupian.

The triangle in Fig. 9 shows the location of five surveys during the period 1978–81. Behringer and Stommel (1980) have published the results of the first of these. The triangle lies astride both y_1 and $\tilde{x}_3(y)$. Comparison of the data from this survey (Figs. 1, 2 and 4 of Behringer and Stommel, 1980) with the results of the model shows general agreement but not in detail. The eastern side of the triangle (right-hand panels of Fig. 2 of Behringer and Stommel) cuts the boundaries nearly perpendicularly. The oxygen minimum between 500 and 1000 m at the southern end

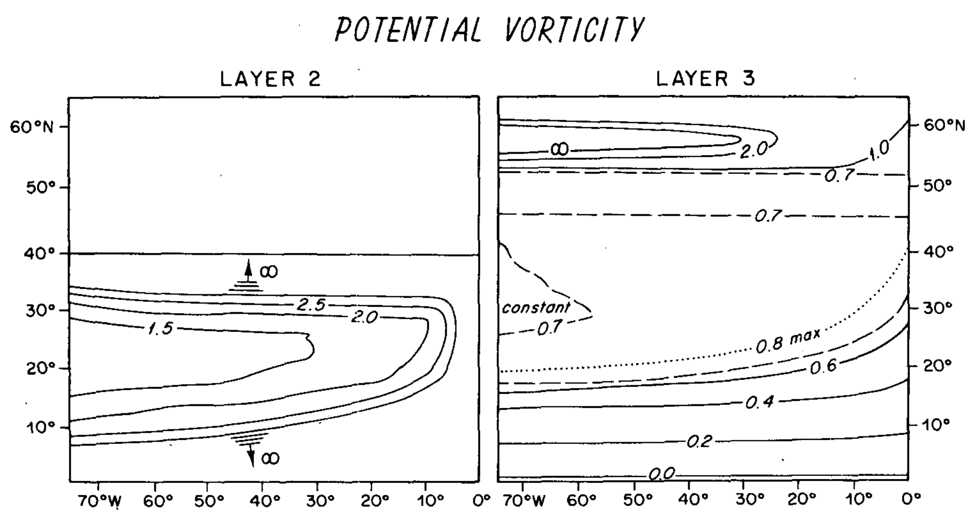

FIG. 12. Potential vorticity in layers 2 and 3 from the model. Units are scaled relative to $2\Omega/1$ km.

of this section seems to correspond to what one might expect from the location of the stagnation region in layer 3. The depth of the bottom of layer 2 in the model is about 250 m, whereas the corresponding depth of the 27.00 isopycnal in the triangle data is about 500 m—a discrepancy that may be due to the closeness to the eastern wall and the stringency of the boundary condition there in the model. The geostrophic velocities relative to 1000 m in layers 2 and 3 computed from the model agree with vertically averaged velocities between 70–250 m and 250–800 m, respectively, as shown in Fig. 4 of Behringer and Stommel within estimated errors.

Acknowledgments. The authors wish to thank the following agencies for their generous support: the Ocean Sciences and Technology Division of the Office of Naval Research (J.L.) and the Atmospheric Sciences (J.P.) and Oceanography (H.S.) sections of the National Science Foundation.

REFERENCES

Behringer, D., and H. Stommel, 1980: The beta-spiral in the North Atlantic subtropical gyre. *Deep Sea Res.*, **27A**, 225–238.

Böhnecke, G., 1936: *Atlas: Temperatur, Salzgehalt und Dichte an der Oberfläche des Atlantischen Ozeans. Deutsche, Atlantische Exped. Meteor, 1925–27, Wiss. Erg.*, Vol. 5, Atlas, 76 pp.

Fuglister, F. C., 1960: *Atlantic Ocean Atlas of Temperature and Salinity Profiles and Data from the International Geophysical Year of 1957–1958. Woods Hole Oceanogr. Inst. Atlas Ser.*, Vol. 1, 200 pp.

Leetmaa, A., and A. F. Bunker, 1978: Updated charts of the mean annual wind stress, convergences in the Ekman layers, and Sverdrup transports in the North Atlantic. *J. Mar. Res.*, **36,** 311–322.

Luyten, J. R., and H. Stommel, 1982: Recirculation reconsidered. *J. Mar. Res.*, **40** (Suppl.), 407–426.

Menzel, D. W., and J. H. Ryther, 1968: Organic carbon and the oxygen minimum in the South Atlantic Ocean. *Deep Sea Res.*, **15,** 327–337.

Rhines, P. B., and W. R. Young, 1981: A theory of the wind-driven circulation. I. Mid-ocean gyres. *J. Mar. Res.*, **40** (Suppl.), 559–596.

Robinson, A. R., and H. Stommel, 1959: The oceanic thermocline and the associated thermohaline circulation. *Tellus*, **11,** 295–308.

Sarmiento, J. L., C. G. H. Rooth and W. Roether, 1982: The North Atlantic tritium distribution in 1972. *J. Geophys. Res.* (in press).

Stommel, H., 1964: Summary charts of the mean dynamic topography and current field at the surface of the ocean, and related functions of the mean wind-stress. *Studies on Oceanography dedicated to Professor Hidaka in commemoration of his sixtieth birthday*, Hidaka Jubilee Committee, Geophysical Institute, University of Tokyo, pp. 53–58.

——, 1979: Determination of watermass properties of water pumped down from the Ekman layer to the geostrophic flow below. *Proc. Nat. Acad. Sci., U.S.*, **76,** 3051–3055.

Sverdrup, H. V., M. W. Johnson and R. H. Fleming, 1942: *The Oceans*. Prentice Hall, 1060 pp.

Veronis, G., 1969: On theoretical models of the thermohaline circulation. *Deep Sea Res.*, **16** (Suppl.), 301–323.

Welander, P., 1959: An advective model of the ocean thermocline. *Tellus*, **11,** 309–318.

——, 1971: The thermocline problem. *Phil. Trans. Roy. Soc. London*, **A270,** 415–421.

Wüst, G., 1935: *Die Stratosphare. Deutsche Atlantische Exped. Meteor 1925–1927, Wiss. Erg.*, Vol. 6, 1 Teil, 2. Lief., 288 pp. English translation, *The Stratosphere of the Atlantic Ocean*, W. J. Emery, Ed., 1978, Amerind, New Delhi, 112 pp.